The Aeronautical Journal (2025), **129**, pp. 2435–2459
doi:10.1017/aer.2025.39

ROYAL AERONAUTICAL SOCIETY

RESEARCH ARTICLE

A comparative study of aerodynamic characteristics of conventional and multi-lobed airships

A. Pai[1] and M. Manikandan[2]

[1]Department of Mechanical and Industrial Engineering, Manipal Institute of Technology, Manipal Academy of Higher Education, Manipal, 576104, Karnataka, India
[2]Department of Aeronautical and Automobile Engineering, Manipal Institute of Technology, Manipal Academy of Higher Education, Manipal, 576104, Karnataka, India
Corresponding author: M. Manikandan; Email: manikandan.m@manipal.edu

Received: 31 July 2024; **Revised:** 26 March 2025; **Accepted:** 1 April 2025

Keywords: airship; conventional; multi-lobed; computational fluid dynamics; aerodynamics

Abstract

Aerodynamic investigations are crucial for the efficient design of Lighter-than-Air (LTA) systems. This study explores the aerodynamic characteristics of conventional and multi-lobed airships, motivated by the growing interest in LTA systems due to advancements in materials science, energy sources, aerodynamics, propulsion technology and control systems. The study employs the k-epsilon turbulence model, which is well-suited for turbulent flow simulations, and the Semi-Implicit Method for Pressure Linked Equations (SIMPLE) algorithm, known for its effectiveness in pressure-velocity coupling in fluid dynamics simulations. The results indicate that multi-lobed airships offer enhanced aerodynamic efficiency over conventional designs. Detailed analyses of lift and drag coefficients provide insights into aerodynamic performance, guiding the optimisation of airship designs for improved efficiency. The findings of this study support the development of more aerodynamically efficient airship designs, which can serve as cost-effective, energy-efficient and quieter alternatives to traditional aircraft, particularly for applications such as surveillance, cargo transport and scientific research.

Nomenclature

A	Coordinates of fins based on hull nose [m];
B	Coordinates of fins based on hull nose [m];
b	Upstream length of computational domain [m];
b_0	Root chord [m];
b_1	Tip chord [m];
C	Coordinates of fins based on hull nose [m];
D	Coordinates of fins based on hull nose [m];
E	Coordinates of fins based on hull nose [m];
F	Coordinates of fins based on hull nose [m];
f	Distance between the center of the lobes [m];
h	Semi-span [m];
l	Downstream length of computational domain [m];
L	Length of the model [m];
SST	Shear stress transport;
V	Envelope volume [m^3];
$Y+$	Dimensionless distance representing the normalized distance of a mesh node from a solid wall;

1.0 Introduction and background

In recent years, there has been a resurgence of interest in airship technology due to its potential for a wide range of applications, including surveillance, cargo transport and scientific research. Airships offer distinct advantages over conventional aircraft, such as superior hovering capabilities and reduced energy consumption for levitation. These attributes make airships an attractive alternative for tasks that require stable, efficient and low-noise flight. Furthermore, their relatively low operational costs and smaller environmental footprint position them as promising candidates for future aerospace solutions.

Advancements in materials science, energy sources, and propulsion technologies have significantly contributed to the revival of airship designs [1]. In particular, the development of multi-lobed airships, those consisting of more than one lobe or section, has generated significant interest. Multi-lobed designs offer several potential benefits over conventional single-lobed airships, including improved stability in the lateral direction, enhanced manoeuverability and increased payload capacity [2–5]. These characteristics make multi-lobed airships particularly suitable for high-altitude scientific exploration, stratospheric observation and long-duration missions.

Despite these promising features, there is a lack of comprehensive studies that compare the aerodynamic performance of conventional and multi-lobed airships [6]. This research aims to fill this gap by conducting a detailed computational analysis of both airship configurations. Using computational fluid dynamics (CFD), we compare the aerodynamic characteristics, specifically the lift and drag coefficients of single-lobed and multi-lobed airships under specified flight conditions. The insights gained from this study will provide valuable information for optimising airship designs to improve aerodynamic efficiency and payload capacity.

The study of airship aerodynamics has evolved significantly over the past few decades, with early research primarily focusing on conventional, single-lobed airships. These investigations laid the groundwork for understanding basic aerodynamic principles, such as the relationship between shape and performance. Early studies examined key factors such as drag, lift and stability, providing a solid foundation for future advancements in airship design. As the field progressed, the focus began shifting toward more advanced airship configurations, particularly multi-lobed designs. Researchers began exploring the potential benefits of multi-lobed airships, which are believed to offer improved stability, increased payload capacity and enhanced maneuverability compared to conventional designs.

Notable early studies on multi-lobed airships have provided compelling evidence of their advantages [7–9]. Despite these promising findings, there remains a lack of direct comparisons of the aerodynamic performance between conventional and multi-lobed airships using experimental setup and advanced computational methods. This gap in research has led to further exploration of the aerodynamic characteristics of these airship configurations using CFD.

Several studies have advanced the design and performance evaluation of airships, incorporating novel methodologies such as genetic algorithms and ant colony optimisation for design optimisation. For instance, Sashi et al. [10] introduced a hybrid method combining genetic algorithms and ant colony optimisation with a meshless CFD solver to enhance airship designs. Liu et al. [11] compared the aerodynamic characteristics of airship hulls with and without fins, providing valuable insights into aerodynamic coefficients and pressure distribution. Additionally, Suman et al. [12] evaluated the performance of the assumed-transition-point criterion with Reynolds-averaged Navier-Stokes (RANS) simulations for lighter-than-air vehicle hulls. Although RANS simulations accurately predicted drag in forced-transition cases, they struggled to match experimental force and moment coefficients in free-transition scenarios. This discrepancy suggests that more advanced simulation methods, such as large eddy simulations (LES), could provide better predictions.

Other significant contributions include Mahzan and Muhamad [13], who analysed various hybrid air vehicle designs using CFD, and Andan et al. [14, 15], who revealed aerodynamic advantages for winged hull airships over conventional designs. Anwar et al. [16, 17] examined the stability of hybrid airships under various wind conditions, while Carrion et al. [18–20] used CFD to enhance understanding of LTA vehicle dynamics and stability. Zhang et al. [21] explored hybrid airships' sensitivity to wind loading, contributing valuable insights into aerodynamic challenges and optimisation strategies.

https://doi.org/10.1017/aer.2025.39 Published online by Cambridge University Press

The use of CFD in the analysis of hybrid and multi-lobed airships has been instrumental in advancing the field. Manideep and Pant [22] used *OpenFOAM* for CFD analysis of single-lobed airship profiles, promoting cost-effective research with open-source tools. Meng et al. [23] provided important insights into hybrid air vehicles using advanced computational methods, while Yueneng et al. [24] applied a biomimetic approach inspired by the Physalia physalis to improve aerodynamic performance in stratospheric airships. More recently, Gupta et al. [25] conducted a comprehensive CFD analysis of the ZHIYUAN-1 airship, emphasising the effectiveness of *OpenFOAM* for detailed LTA system investigations.

The impact of environmental factors, such as wind gusts, on airship performance has also been a focus of recent research. Sasidharan et al. [26, 27] studied the effects of wind gusts on the ZHIYUAN-1 airship using CFD simulations, highlighting the need for designs that can withstand fluctuating wind conditions. Similarly, Magar et al. [28] validated OpenFOAM's ability to predict aerostat envelope performance, with results aligning well with experimental data.

CFD has also been applied to examine the thermal performance of airships equipped with photovoltaic module arrays (PVMA). Zhang et al. [29] proposed thermal models for high-altitude hybrid airships, analysing temperature and velocity distributions within internal helium. In another study, Zhang et al. [30] explored mission-based multidisciplinary optimisation of solar-powered hybrid airships, coupling CFD with optimisation algorithms like NSGA-II to explore design trade-offs at various altitudes. These studies underscore the importance of CFD in optimising both the aerodynamic and thermal efficiency of airships, particularly in missions requiring sustainable energy sources.

Experimental validation continues to play a crucial role in confirming the accuracy of CFD predictions. Several studies have provided experimental data to validate CFD models. For example, Funk et al. [31] conducted aerodynamic tests on an airship's hull-fin region, creating a data set for CFD code validation. Ping et al. [32] measured aerodynamic forces and coefficients in a wind tunnel, comparing these results with numerical simulations. Sam et al. [33] provided wind-tunnel data for multi-lobed hybrid airship geometries, revealing that higher drag due to lift was observed compared to existing models, although lift curve slopes aligned well with theoretical predictions. These experimental studies provide essential data to refine and validate CFD models.

The role of fins in enhancing the directional stability of airships has also been explored in numerous studies. Cui et al. [34] investigated the effects of fin shape and location, finding that cross-type fins provide superior aerodynamic performance. Jefferson et al. [35] discussed the challenge of validating numerical solutions with wind tunnel results, particularly during the early stages of design. Alireza et al. [36] used CFD to study the roll damping coefficient, while Sohan et al. [37, 38] proposed a systematic approach for designing airship fins using constrained optimisation, validated through wind tunnel experiments.

Finally, the choice of turbulence model is critical in obtaining accurate CFD results for airship aerodynamics. Several studies have compared different turbulence models, including standard high Reynolds k-ε, LES and VMS-LES, for their ability to replicate real-world conditions. Voloshin et al. [39] found that the SA model was most suitable for small to medium angles of attack in conventional airships, while Kamal et al. [40, 41] evaluated LES and VMS-LES models for a prolate ellipsoid and found the latter most effective for high angles of attack. Wu et al. [42] showed that the SST k-ω and Realizable k-ε models outperformed the SA model for high angles of attack. Kanoria et al. [43] demonstrated that LES models outperform RANS models for the ZHIYUAN-1 airship, emphasising the trade-offs between model accuracy and computational cost.

This study seeks to address the gap in the literature by leveraging CFD to simulate and compare the aerodynamic performance of conventional and multi-lobed airship designs. By employing reliable turbulence models and numerical algorithms, this research aims to provide a more comprehensive understanding of the aerodynamic characteristics of these airship configurations under specified flight conditions.

The remainder of this paper is organised as follows: section 2.0 discusses the need for the present study. Section 3.0 details the methodology, including the generation of envelope shapes, computer-aided

https://doi.org/10.1017/aer.2025.39 Published online by Cambridge University Press

models for simulations and the fin geometry. Section 4.0 outlines the simulation specifics, covering flow conditions, solver setup, turbulence model, computational domain and grid. Section 5.0 presents the model validation with experimental data from the literature, grid independence study, comparison of turbulence models, domain sensitivity analyses, a comparative study on the aerodynamics of conventional and multi-lobed configurations and flow field description results. Finally, section 6.0 concludes the paper with an analysis of the results.

2.0 Need for the present study

While there have been studies utilising CFD to demonstrate the flow characteristics of conventional and multi-lobed airships and to predict their aerodynamic and stability properties, a comprehensive comparison remains unexplored. Tripathi et al. [44] compared the aerodynamic performance of conventional and tri-lobed configurations made with the LOTTE profile. Carrion et al. [18–20] investigated the aerodynamics of bi-lobed models, similar in shape to the Airlander 10 airship by Hybrid Air Vehicles Ltd., and tri-lobed models resembling the Airlander 50 airship. However, to the best of the authors' knowledge, a CFD study comparing the aerodynamic characteristics of conventional, bi-lobed and tri-lobed airship configurations across various angles of attack has not been presented in the literature.

In this study, standard profiles such as ZHIYUAN-1, Wang, NPL, Ellipsoid, Garg and LOTTE were employed to create envelope profiles for both conventional and multi-lobed airship models. To ensure a fair comparison, all models were designed with the same envelope volume and simulated under identical flow conditions. Additionally, the study examined the impact of fins and gondola on the flow field and the aerodynamic characteristics, specifically lift and drag, of the airships.

Turbulence modeling is crucial in most CFD simulations, as virtually all engineering applications are turbulent and thus require an appropriate turbulence model. The implementation of the turbulence model within the numerical scheme significantly influences the simulation results. Most existing studies on aerodynamic performance often select a single turbulence model from the simulation software, leading to variability in results due to differences in simulation objects and fluid characteristics. Given the absence of a uniform standard for selecting turbulence models, simulation outcomes can diverge from actual conditions. Therefore, selecting the appropriate turbulence model is vital for achieving agreement between simulation results and real-world conditions. This study aims to compare the effects of different turbulence models on validated outcomes.

3.0 Geometry description

This section explores a detailed description of the geometries pertinent to the present study. Understanding the geometric parameters is crucial for accurate modeling and analysis. This comprehensive overview ensures that the conditions of the present study are replicable and that the results are interpretable within the defined parameters.

3.1 Envelope shape generation

The current study is based on the standard profiles of six airships shown in Fig. 1, viz., ZHIYUAN-1, LOTTE, Ellipsoid, Garg, Wang and NPL. In this study, the Gertler Series 58 shape generator [45, 46] has been considered for airship envelope generation. A detailed description of the shape generator and its associated design factors can be found in the existing literature [47, 48]. To obtain the final envelope surface, the curve is revolved around the desired axis to produce the axisymmetric shape of the body. The multi-lobed shape can be considered as several conventional bodies as shown in Fig. 2.

Figure 3 illustrates the fundamental method for determining the necessary length of a specific shape to achieve a desired envelope volume, ensuring consistent volume across all models utilised in the simulation. All the models used in this study are rigid. The effects of the airship's flexible nature, which

https://doi.org/10.1017/aer.2025.39 Published online by Cambridge University Press

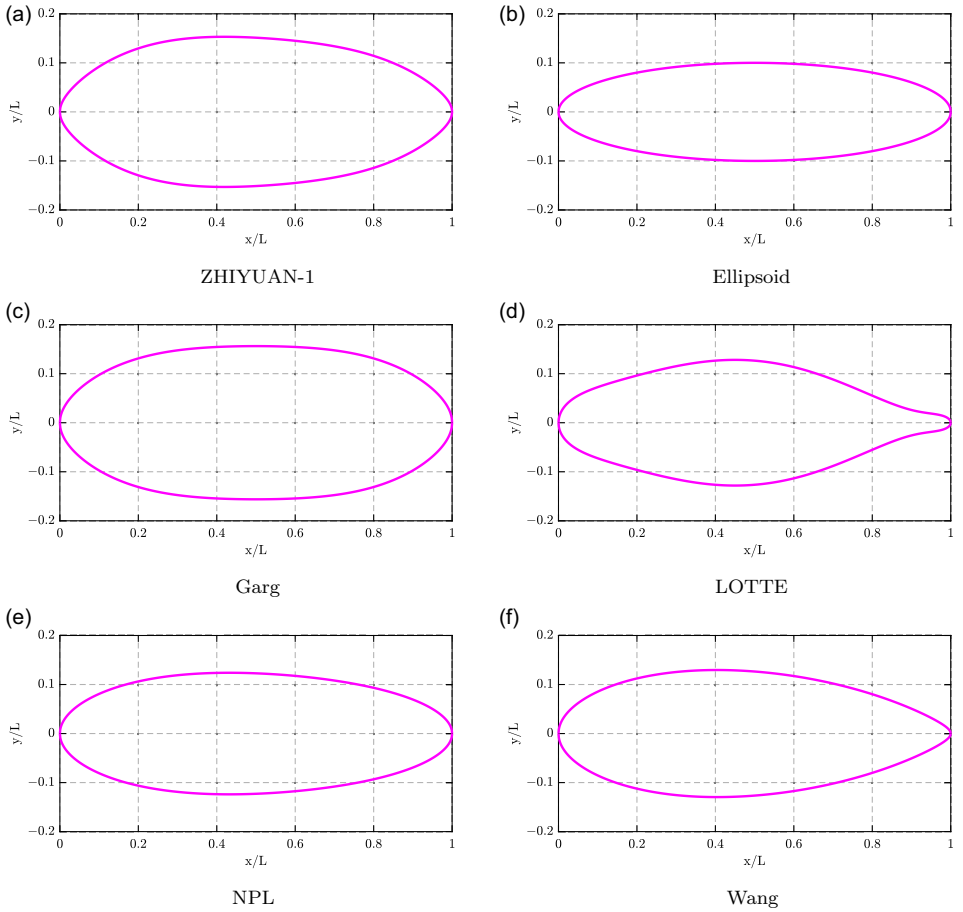

Figure 1. *Standard envelope profiles of airships.*

leads to fluid-structure interaction, are beyond the scope of this study. This study encompasses not only the airship hull but also the geometries of the fins and gondola for conventional models. For the bi- and tri-lobed configurations, simulations were conducted using the hull in conjunction with the fins.

3.2 Airship models

To ensure the accuracy of the CFD simulations, a rigorous validation process was implemented in this study. This process involved a comparative analysis between the numerical results for the ZHIYUAN-1 airship model shown in Fig. 4 and the experimental wind tunnel data presented in a prior study [49]. Meticulous attention was given to replicating the 3D model of the ZHIYUAN-1 to accurately reflect the dimensions of the physical model used in the wind tunnel experiments. This dimensional precision was critical for establishing a reliable benchmark for the CFD simulations. The geometric details of the CAD model are listed in Table 1.

Constructing a multi-lobed airship requires a detailed design and modeling process to optimise both aerodynamic performance and structural integrity. Using *SOLIDWORKS*® CAD software, the airship's envelope is created by importing shape coordinates and employing the revolve feature to form the smooth, curved hull. The gondola, which houses essential equipment and serves as the control and propulsion centre, is modeled by sketching its dimensions and extruding the sketch along the mid-plane. The fins, crucial for stabilisation, are designed with precise sketches based on specified dimensions

https://doi.org/10.1017/aer.2025.39 Published online by Cambridge University Press

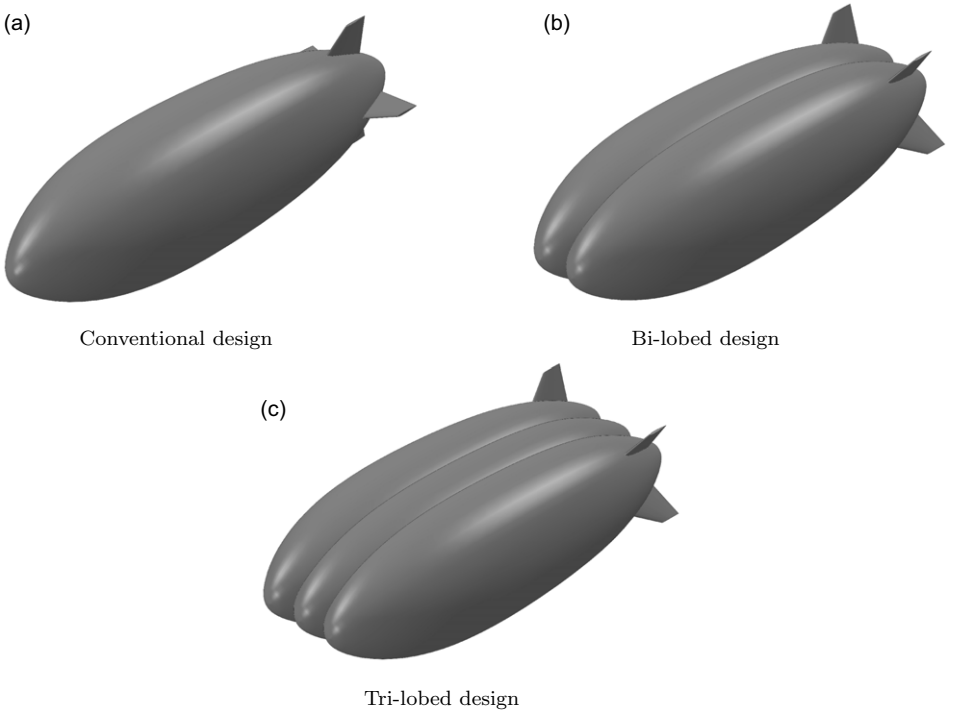

Figure 2. *Different airship configurations.*

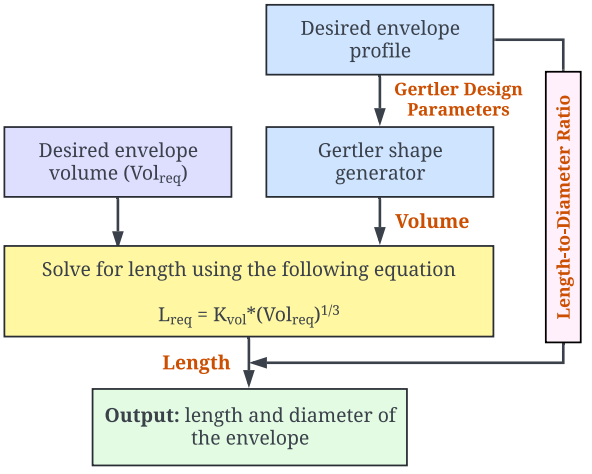

Figure 3. *Procedure for envelope sizing.*

Figure 4. *Scaled CAD model of the ZHIYUAN-1.*

https://doi.org/10.1017/aer.2025.39 Published online by Cambridge University Press

Table 1. *Geometry specifications of the ZHIYUAN-1 model*

Parameter	Value
Length (m)	1.83
Maximum diameter (m)	0.55
Fineness ratio (–)	3.3
Envelope volume (m^3)	0.2935
Surface area (m^2)	2.5701
Reference area (m^2)	0.4416
Reference length (m)	1.83
Volume Reynolds number (–)	2.58×10^6

Table 2. *Specifications of fin geometry [49]*

Parameter	Values, [m]
Root chord (b_0)	0.1617
Tip chord (b_1)	0.0936
Semi-span (h)	0.1504
Leading edge sweep angle (°)	40
Coordinates of fins measured from hull nose	
A	(1.5618, 0.1748)
B	(1.6655, 0.1368)
C	(1.7233, 0.1368)
D	(1.7496, 0.2872)
E	(1.7174, 0.2872)
F	(1.6560, 0.2872)

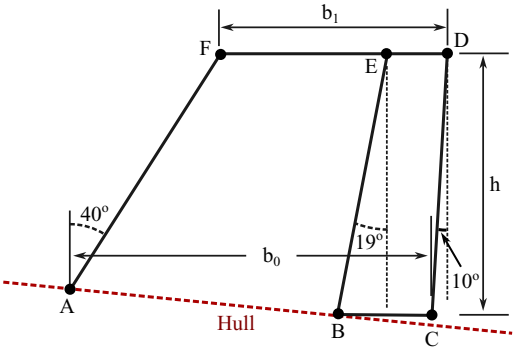

Figure 5. *Reference sketch of an airship fin (Reproduced from (49)).*

shown in Fig. 5. The sketches are lofted to replicate the aerodynamic profile of the fins accurately. The geometrical parameters of the fins are given in Table 2.

In this study, a standardised methodology was applied to all airship profiles. Initially, 3D models of single-lobed configurations shown in Fig. 6 were generated, ensuring a uniform hull volume for each model. To enable a thorough aerodynamic comparison, bi-lobed and tri-lobed models were subsequently developed using the parametric design methods detailed in the study [48]. By maintaining a constant volume across all configurations, the study focused on evaluating the aerodynamic performance variations attributable to different lobe configurations.

https://doi.org/10.1017/aer.2025.39 Published online by Cambridge University Press

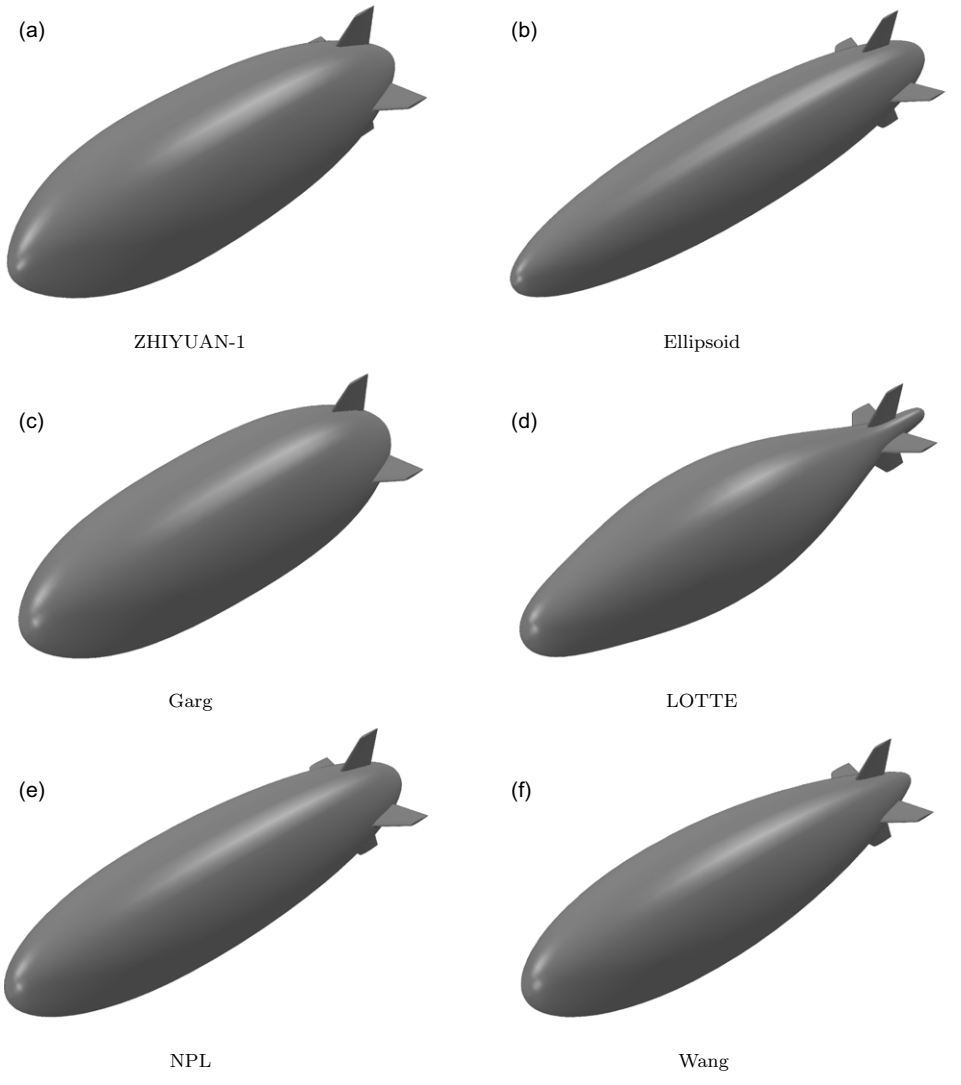

Figure 6. *Single-lobed (conventional) airship models with fins.*

To achieve the objective, fins were integrated into the airship designs. The NACA 0010 aerofoil profile shown in Fig. 7 was selected for these fins due to its well-documented aerodynamic properties. The aerodynamic characteristics of NACA 0010 are presented in Fig. 8 obtained from the dataset of aerofoils provided by Kanak et al. [50]. Different fin configurations were employed for single-lobed and multi-lobed airships during the modeling process. The single-lobed models featured a cross-type fin configuration, whereas the multi-lobed variants utilised a more complex 'X-configuration' as shown in Fig. 2. In the case of both aircraft and airships, the sizing of tail fins is typically performed using a method known as the tail volume coefficient approach [51], which is based on historical data. The tail volume coefficient is a function of the envelope volume. Since the envelope volume is identical for all models considered in the present study, a uniform tail fin size is applied across all the models.

To establish a uniform reference for performance evaluation, a standardised methodology for calculating key aerodynamic parameters was employed. The reference length for each airship was computed

https://doi.org/10.1017/aer.2025.39 Published online by Cambridge University Press

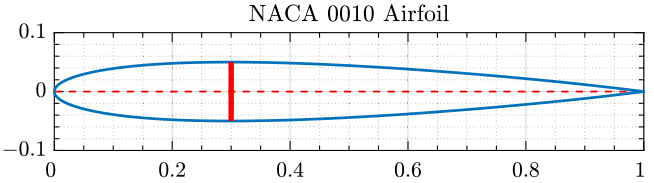

Figure 7. *Schematic of the NACA 0010 aerofoil.*

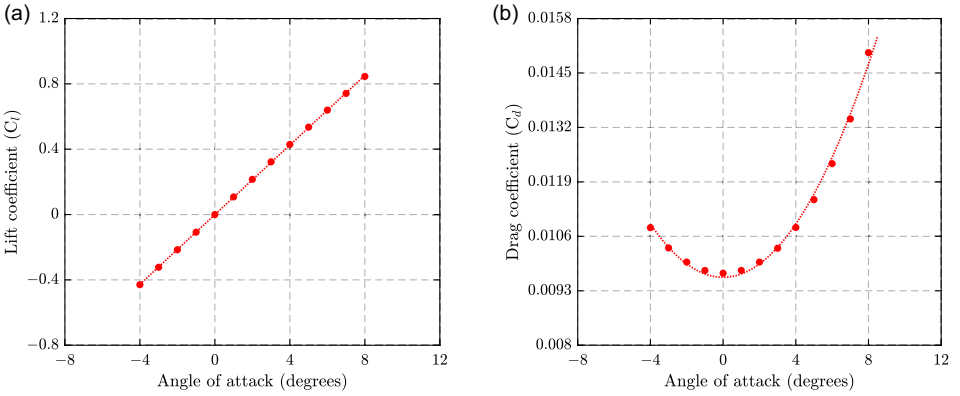

Figure 8. *Aerodynamic characteristics of the NACA 0010 at* $Re = 2.58 \times 10^6$.

using the formula $V^{1/3}$, and the reference area was determined using the formula $V^{2/3}$, where V represents the volume of the hull containing the lifting gas. Importantly, the value of V was held constant across all airship models, facilitating direct comparison of aerodynamic performance metrics such as lift and drag coefficients. This meticulous approach resulted in a robust and well-defined framework for comparative analysis.

4.0 Simulation setup

This section outlines the governing equations, flow conditions, computational domain, boundary conditions, meshing topology and flow solver settings used in the simulations.

4.1 Governing equations

The present study utilised *ANSYS* Fluent 2023 and *OpenFOAM*® for numerical simulations of airship aerodynamics, focusing on a three-dimensional, steady-state, incompressible flow. The use of *OpenFOAM* flow solver in the present study is motivated by two main reasons: first, to validate the results obtained from *ANSYS* Fluent, and second, to overcome computational limitations related to the number of cells/elements available during the meshing of the computational domain under the academic license of *ANSYS* Fluent (Fluent can handle up to 512 k cells). Mathematically, any three-dimensional flow can be described by a set of five non-linear differential equations, which are intricately coupled and highly complex to solve [25, 52]. These equations are known as the Navier-Stokes equations, and they are divided into one mass continuity equation (Equation 1), three momentum conservation equations (Equation 2), and one energy conservation equation (Equation 3).

Mass Continuity:

$$\frac{\partial \rho}{\partial t} + \frac{\partial}{\partial x_j}\left[\rho u_j\right] = 0 \tag{1}$$

https://doi.org/10.1017/aer.2025.39 Published online by Cambridge University Press

Table 3. *Flow conditions for CFD simulations*

Parameter	Value
Freestream velocity, V_∞ (m/s)	60.39
Freestream temperature, T_∞ (K)	298.15
Turbulence intensity, I (%)	0.10
Mach number, M_∞ (–)	0.18
Volumetric Reynolds number, Re_v (–)	2.58×10^6
Angle-of-attack, α (°)	$0, \pm 5, \pm 10$

Equations of Motion:

$$\frac{\partial}{\partial t}(\rho u_i) + \frac{\partial}{\partial x_j}\left[\rho u_i u_j + p\delta_{ij} - \tau_{ij}\right] = 0, \quad i = 1, 2, 3 \tag{2}$$

Energy Conservation:

$$\frac{\partial}{\partial t}(\rho e_0) + \frac{\partial}{\partial x_j}\left[\rho u_j e_0 + u_j p + q_j - u_i \tau_{ij}\right] = 0 \tag{3}$$

where t represents the time variable. The variables x_i and u_i refer to the i^{th} components of the spatial and velocity vectors, respectively. The symbols ρ, p, and τ stand for density, pressure and viscous shear stress, respectively. The total energy is represented by e_0, and the heat flux is denoted by q.

The steady-state values for flow variables such as velocity and pressure in the present study were determined using the RANS equations. These equations replace the original flow variables in the Navier-Stokes equations with the sum of their time-averaged values and fluctuating components.

4.2 Flow conditions

The present study utilised flow conditions consistent with the experimental testing conducted by Wang et al. [49] on the airship model with ZHIYUAN-1 profile. This approach ensures alignment between computational and experimental results, thereby facilitating the validation of the CFD analysis. By maintaining uniform flow conditions across all airship analyses, the study enables fair comparisons between different designs. The flow conditions are summarised in Table 3.

4.3 Computational domain

A domain sensitivity study in CFD ensures simulation accuracy by analysing how domain size and configuration affect results shown in Fig. 9. By varying upstream/lateral length (b) and downstream length (l) relative to a reference length (L), optimal sizes were identified. Results showed that $b = 6L$ and $l = 12L$ minimised error to 2.08%, balancing accuracy and computational resources.

The cylindrical computational domain shown in Fig. 10 selected for simulating airflow around an airship offers several advantages, including efficient representation of the flow field and minimised computational complexity. Extending boundaries $6L$ upstream, $12L$ downstream and $6L$ laterally ensures a sufficiently large region to capture wake and boundary layer interactions. To enhance mesh resolution near the airship, a body of influence (BOI) with dimensions $1.5L \times 0.6L \times 0.6L$ was used. This localised refinement allows for finer meshing in critical areas, accurately capturing flow details like boundary layer separation and wake formation while maintaining computational efficiency in less critical regions. Leveraging the axisymmetric nature of the airship, the mesh was generated for only half the body, reducing computation time while still capturing essential flow characteristics.

Adiabatic no-slip conditions were applied to the airship surfaces, ensuring airflow adherence and no heat transfer. Pressure far-field boundary conditions were used for the inlet, outlet, and far-field regions, simulating unobstructed airflow and consistency with atmospheric conditions. This approach, with its

https://doi.org/10.1017/aer.2025.39 Published online by Cambridge University Press

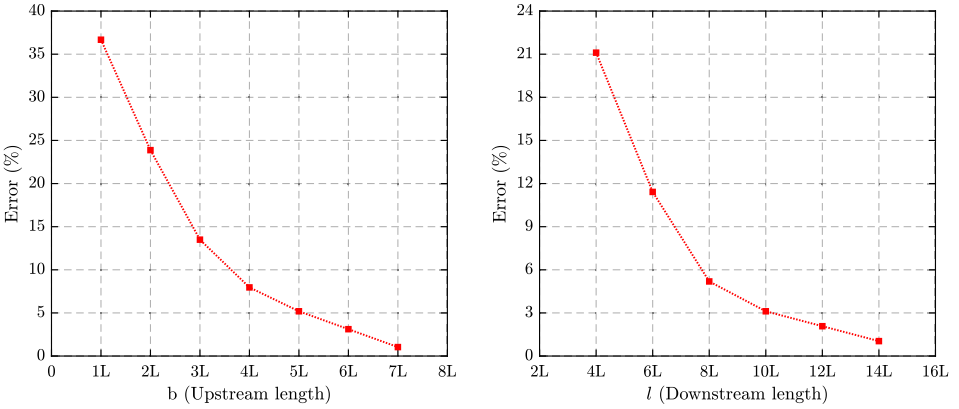

Figure 9. *Sensitivity analysis of the computational domain.*

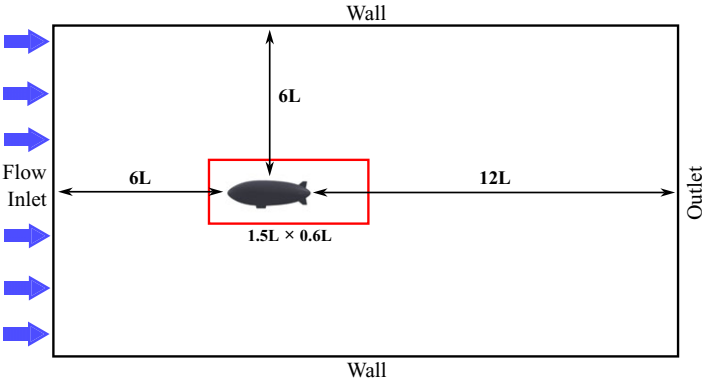

Figure 10. *Computational domain used for the simulation.*

tailored computational domain, mesh refinement and boundary conditions, ensures accurate simulation of aerodynamic interactions around the airship while optimising computational efficiency, enabling effective analysis and design optimisation.

4.4 Mesh generation

The simulated flow includes low subsonic speeds (Mach number < 0.2) and high volumetric Reynolds number (Re_v) characteristics. These conditions cause boundary layer variations and flow separation, leading to eddies and vortices that significantly impact the overall aerodynamics. Therefore, designing an appropriate mesh to accurately capture these complex flow variations was the most challenging and crucial step in the current numerical investigations. A poly-hexcore mesh was generated using *ANSYS* Fluent meshing for its efficiency and superior gradient approximation, which is crucial for airship aerodynamics. This mesh topology reduces the overall mesh count compared to tetrahedral or polyhedral meshes, enhancing computational efficiency and resource management. The poly-hexcore mesh minimises numerical diffusion, preserving flow feature sharpness and simulation fidelity. Refinement was focused near airship walls and fins to accurately capture curvature and thin trailing edges without excessive computational costs. To capture boundary layer flow variations, 34 inflation layers were projected with a growth rate of 1.2 and an initial layer height of 1.33e-5 m leading to a total inflation layer thickness of 2.93e-2 m. The final mesh had around 2.4 million elements, a maximum skewness of 0.54, minimum orthogonal quality over 0.1, and an average Y+ value under 1. Figure 11 shows the fine mesh for the

https://doi.org/10.1017/aer.2025.39 Published online by Cambridge University Press

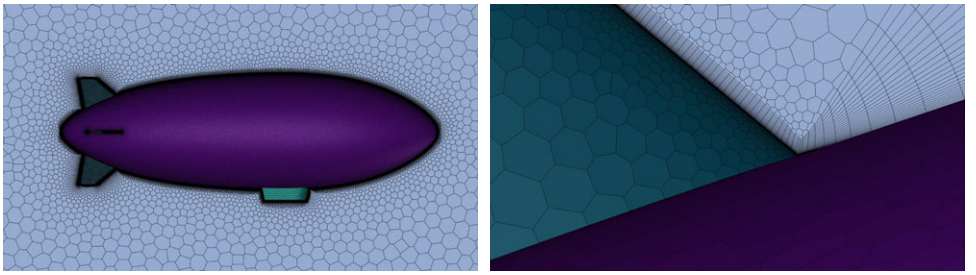

Figure 11. *Schematic of the discretised flow domain.*

analysis setup displaying the resolution of the curved surfaces, boundary layer growth, and the finer mesh near the airship.

4.5 Solver setup

The SIMPLE algorithm was applied for pressure-velocity coupling in the simulation, ensuring stable and reliable solutions for fluid dynamics problems. The k-ε standard turbulence model was selected for its balance between computational efficiency and accuracy in capturing flow characteristics, validated through a comparative study with Spalart-Allmaras (SA) and SST k-ω models. The rationale for choosing the k-ε turbulence model is explained in Section 5.2. Convergence was achieved when normalised residuals were reduced by five orders of magnitude, ensuring solution stability. This framework provides a rigorous basis for analysing airship aerodynamics.

5.0 Results and discussions

5.1 Grid selection study

To reduce the computational cost, grid selection studies are essential in airship aerodynamics. Airships operate across various flow regimes, requiring robust simulations for accurate performance predictions. To assess grid convergence, this analysis compares three levels of grid refinement for the ZHIYUAN-1 shaped hull with fins and gondola configuration. The first grid, being coarse, consisted of 0.9 million elements. The second, a finer grid, had 2.4 million elements. The third and finest grid included 4 million elements. Comparing the drag coefficient values of the ZHIYUAN-1 airship at a 0° angle-of-attack showed that fine and very fine meshes provided better results shown in Fig. 12, indicating solution convergence. A fine mesh with 2.4 million elements was employed for all simulations of the conventional models, resulting in a 6.8% error at a zero-degree angle-of-attack for the ZHIYUAN-1 model when compared to experimental data. This mesh strikes a balance between computational cost and accuracy, thereby validating the CFD analysis and ensuring reliable results for airship performance evaluation. The simulations were conducted on a computer with a 12th-generation Intel Core i7 processor (14 cores) and 16 GB of RAM.

5.2 Comparison of turbulence models

In this study three turbulence models were compared, namely Spalart-Allmaras [53, 54], SST k-ω [55, 56] and k-ε [57, 58] to ensure accurate and reliable CFD simulations for airship aerodynamics. The aerodynamic data from these models were compared with experimental results from wind tunnel testing on the ZHIYUAN-1 airship to identify the most suitable model for predicting flow behaviour and aerodynamic characteristics. Figure 13 illustrates the performance of each turbulence model in capturing

https://doi.org/10.1017/aer.2025.39 Published online by Cambridge University Press

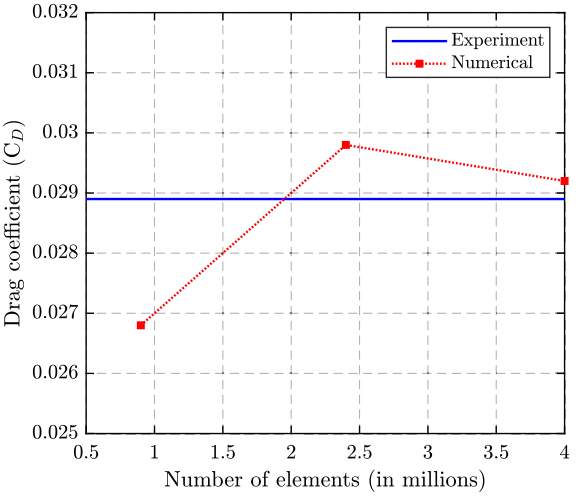

Figure 12. *Grid selection test.*

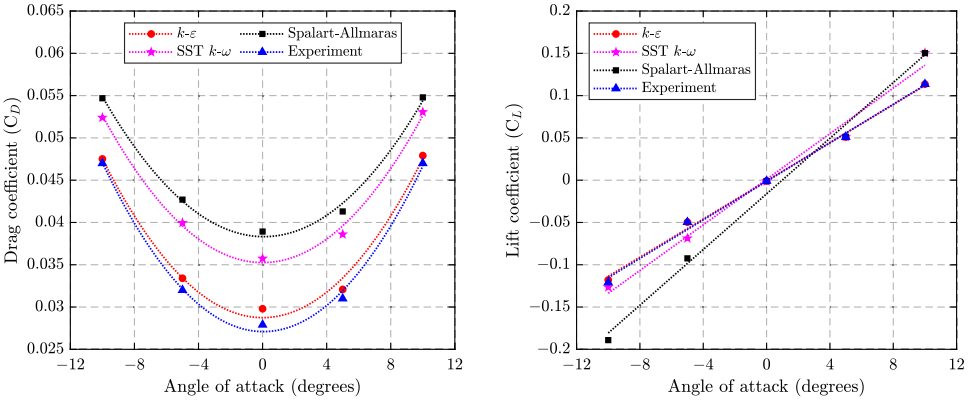

Figure 13. *Comparison of different turbulence models.*

key aerodynamic parameters, such as lift and drag coefficients, across various angles of attack. The standard k-ε turbulence model outdid the others in accurately predicting flow behaviour and aerodynamic characteristics.

The SST k-ω model, while estimating lift coefficients adequately, consistently reported higher drag values compared to the other models and experimental data. This discrepancy is attributed to premature estimating of the transition point from laminar to turbulent flow, affecting overall drag estimation. In contrast, the k-ε model demonstrated superior performance in predicting both lift and drag coefficients, closely aligning with experimental data. Its consistent performance led to its selection for further analysis. The comparison underscores the importance of choosing the right turbulence model for accurate CFD simulations of airship aerodynamics. The k-ε model's selection ensures confidence in the predictive capabilities of the simulations, paving the way for further analysis and optimisation of airship designs.

5.3 Validation with experimental data

Validation with experimental data is a crucial step in ensuring the accuracy and reliability of CFD simulations for airship aerodynamics. This study compares numerical solutions with experimental data

https://doi.org/10.1017/aer.2025.39 Published online by Cambridge University Press

Table 4. *Geometric dimensions of conventional configurations*

Profile	Hull Length (m)
ZHIYUAN-1	1.83
Ellipsoid	2.41
Garg	1.77
LOTTE	2.22
NPL	2.08
Wang	2.09

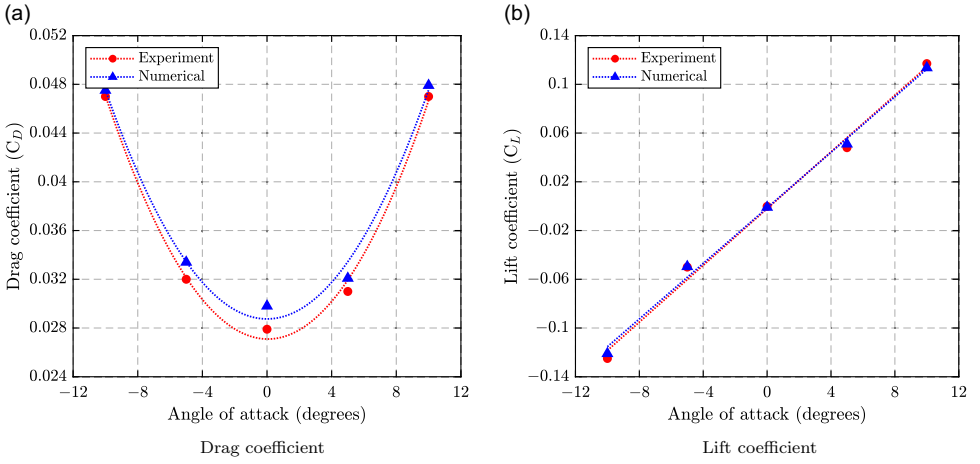

Figure 14. *Validation of CFD results for ZHIYUAN-1 against experimental data from (49).*

obtained from controlled wind tunnel tests [49] to evaluate the congruence between simulated and real-world aerodynamic behaviours. Figure 14 illustrates a detailed comparison between the numerical predictions and experimental data, demonstrating a high degree of correlation. A thorough analysis revealed that the maximum deviation between the numerical and experimental results was 6.8% at a zero-degree angle-of-attack and an average error of 3%, indicating a good agreement between the simulated and experimental aerodynamic characteristics of the airship. The numerical results from CFD, presented in Fig. 14, were obtained using the k-ε turbulence model.

5.4 Numerical results

The analysis focuses on key aerodynamic coefficients, particularly lift and drag, crucial for airship performance and efficiency. Lift combines buoyancy, influenced by the density difference between lifting gas and air, and aerodynamic lift, affected by the airship's shape. Drag, opposing the airship's motion, impacts thrust requirements, efficiency and fuel consumption. Minimising drag is essential for better endurance. The analysis compares various airship configurations by examining these coefficients, aiding in design optimisation for specific operational needs and conditions. This serves as a foundational step in enhancing airship performance and efficiency.

5.4.1 Aerodynamic performance of conventional and multi-lobed airships

The geometric data has been calculated for the specified envelope volume of 0.2935 m^3, and the results are presented in Table 4.

https://doi.org/10.1017/aer.2025.39 Published online by Cambridge University Press

Table 5. *Comparison between Ansys Fluent and OpenFOAM*

Profile	Average Error (%)
ZHIYUAN-1	3.88
Ellipsoid	3.53
LOTTE	2.02
NPL	1.47
Wang	1.76
Garg	2.23

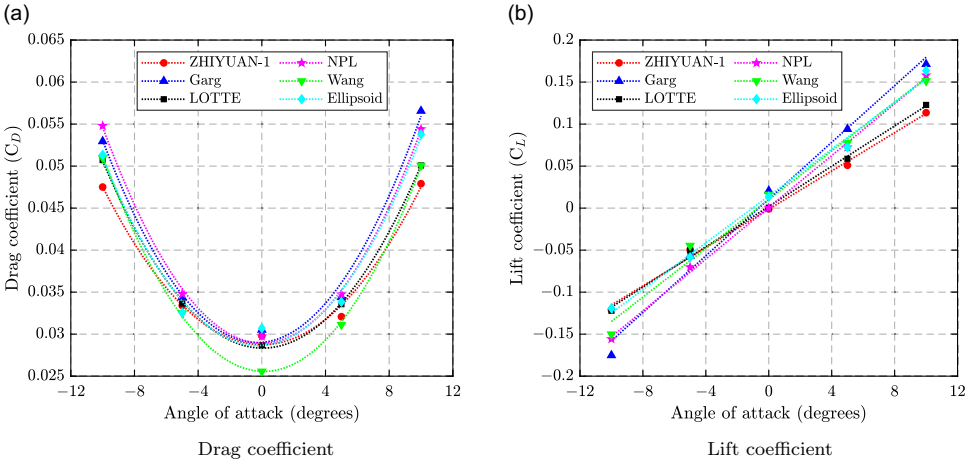

Figure 15. *Aerodynamic characteristics of conventional airships.*

Figure 15 illustrates the changes in aerodynamic parameters for conventional airships as the angle-of-attack (AoA) varies from -10° to 10°. These angles were chosen to encompass all possible flight scenarios for the airship.

After validating the solver's ability to capture aerodynamic coefficients for the conventional (single-lobed) ZHIYUAN-1 model with fins and gondola using experimental data [49], additional verification was performed on other airship models, including fins and gondola. Comparative analyses using *Fluent* and *OpenFOAM* software under identical flow conditions showed that the results from both software were in good agreement shown in Fig. 16. This confirmed the reliability and accuracy of the CFD simulations. The average error percentages between the data obtained from the two different solvers are shown in Table 5. *OpenFOAM*® is an open-source CFD software developed by OpenCFD Ltd. since 2004. It offers flexible solvers for various engineering applications, including compressibility, turbulence, thermal, chemical reactions, solid mechanics and electromagnetic fluctuations. *OpenFOAM* includes tools for pre-processing (blockMesh, snappyHexMesh), solving, and post-processing (ParaView). It supports parallel processing, reducing time and memory constraints, and allows custom solver design.

The comparison between simulation data and experimental results for the ZHIYUAN-1 model, including fins and gondola, as presented in Fig. 14, indicates that the domain size, mesh settings and boundary conditions employed in *ANSYS* Fluent are well-suited for models featuring fins and gondola. However, these settings were found to be inadequate for accurately capturing the flow behaviour over the bare hull. As shown in Fig. 17, there is a significant discrepancy between the results obtained from Fluent and *OpenFOAM*. The *OpenFOAM* simulations for the bare hull exhibit a strong agreement with experimental data, with an error of approximately 7.7%, significantly outperforming Fluent, which shows

https://doi.org/10.1017/aer.2025.39 Published online by Cambridge University Press

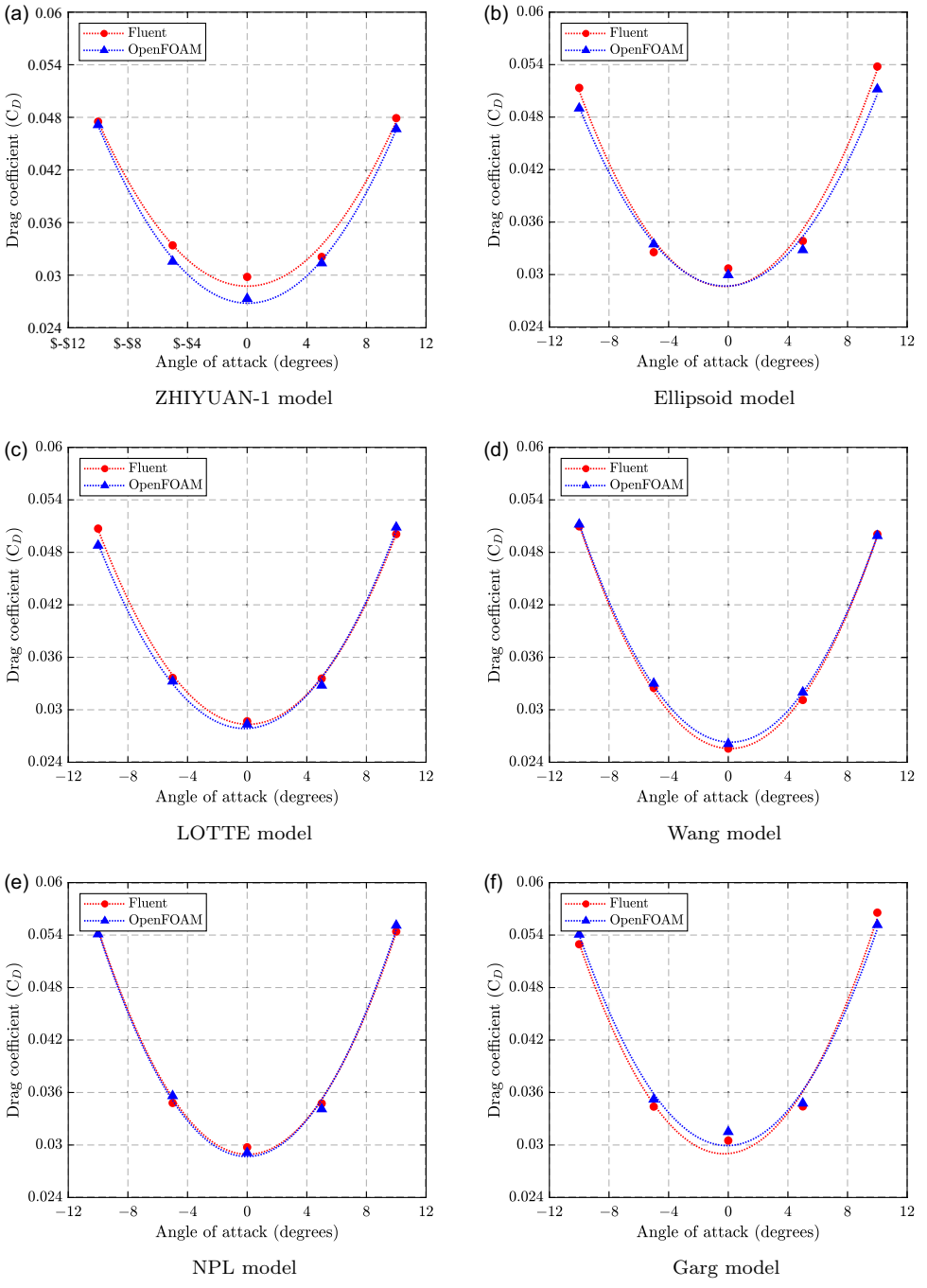

Figure 16. *Comparison of simulation results between Fluent and* OpenFOAM.

much larger deviations. Consequently, *OpenFOAM* was chosen to predict the aerodynamic characteristics of bare hull models for all profiles. The simulations were performed using a mesh setup shown in Fig. 18 consisting of 6.1 million hexahedral cells. SnappyHexMesh was selected for mesh generation due to its reliable method for defining final layer thickness and its robust control over the meshing process. The SimpleFoam solver, coupled with the k-epsilon turbulence model, was employed for all simulations.

https://doi.org/10.1017/aer.2025.39 Published online by Cambridge University Press

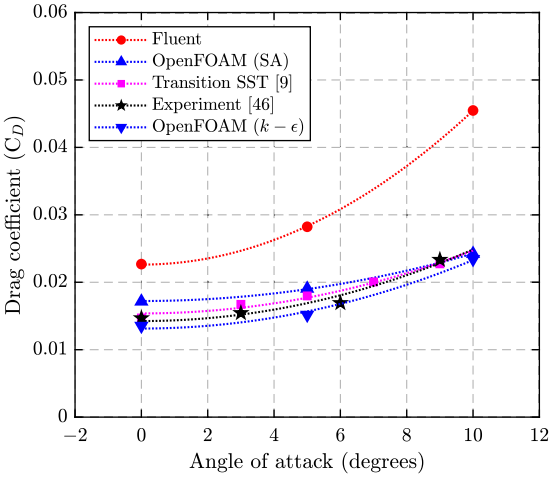

Figure 17. *Variation of drag coefficient with angle-of-attack for the bare hull of the ZHIYUAN-1 model.*

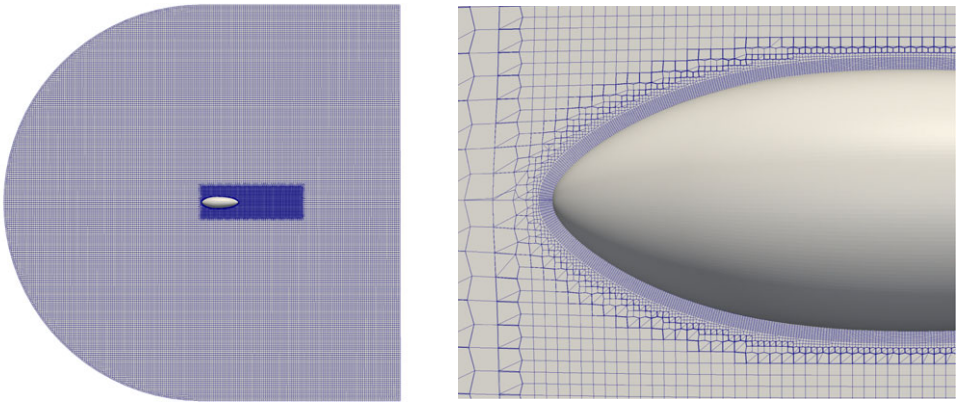

Figure 18. *Schematic of the discretised computational domain used in* OpenFOAM.

Standard Dirichlet and Neumann boundary conditions, appropriate for steady incompressible flow, were applied across all cases. The solver operates using the SIMPLE algorithm. To ensure stability and convergence, the solver was relaxed with a pressure relaxation factor of 0.3 and a relaxation factor of 0.7 for both momentum and turbulence variables. This relaxation strategy helps to mitigate residuals, preventing divergence and enhancing the stability of the solution. All simulations were iterated until the pressure, momentum and turbulence residuals were reduced to a threshold of 1e-5. The initial conditions for the simulation setup in *OpenFOAM* are identical to those used in Fluent (refer to Table 3).

The impact of the gondola and fins was also analysed by comparing three configurations: hull alone, hull with fins and hull with both fins and a gondola. The results presented in Fig. 19 indicated that excluding the gondola reduced the drag coefficient by $3-17\%$, and excluding the fins resulted in a $47-53\%$ reduction in drag coefficient.

5.4.2 Aerodynamic comparison of multi-lobed profiles

The study also compared bi-lobed and tri-lobed configurations presented in Fig. 20 for the specified envelope volume. All simulations for the bi-lobed and tri-lobed models were conducted using *OpenFOAM*. The geometric dimensions were adjusted to maintain a constant volume across all configurations. For an envelope volume of ($\mathrm{V} = 0.2935\ m^3$), the geometric values are provided in Table 6, where f denotes

https://doi.org/10.1017/aer.2025.39 Published online by Cambridge University Press

Table 6. *Geometric dimensions of the multi-lobed configuration*

Profile	Hull Length (m)		f (m)	
	Bi-lobed	Tri-lobed	Bi-lobed	Tri-lobed
ZHIYUAN-1	1.62	1.48	0.1487	0.1360
Ellipsoid	2.13	1.95	0.1280	0.1171
Garg	1.57	1.43	0.1464	0.1340
LOTTE	1.96	1.79	0.1505	0.1373
NPL	1.84	1.68	0.1379	0.1261
Wang	1.85	1.69	0.1435	0.1311

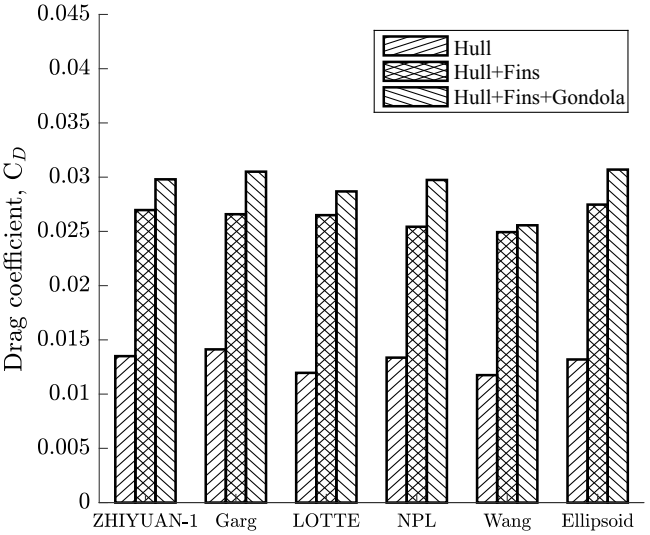

Figure 19. *Impact of gondola and fins on the drag characteristics of conventional airships.*

the lateral distance between the two lobes. The value of f is assumed to be 0.3 times the diameter of a lobe (D), represented as $f = 0.3 \times D$. The data shown in Figs. 21a and b suggest that the fins are the main contributors to the increased drag, which increased drag coefficient by $28 - 57\%$ for bi-lobed models and $22 - 54\%$ for tri-lobed models.

Both the bi-lobed and tri-lobed models exhibit similar aerodynamic efficiencies shown in Fig. 22 across the different profiles. The main difference lies in the slight variations in lift-to-drag ratios at different angles of attack, with the tri-lobed model showing slightly better performance at lower angles.

5.4.3 Aerodynamic comparison of conventional and multi-lobed airships

The drag polar plots presented in Fig. 23 for the conventional, bi-lobed and tri-lobed configurations indicate that the tri-lobed model exhibits a superior lift-to-drag ratio (L/D_{max}) compared to both the single-lobed and bi-lobed models.

A collective drag polar plot, presented in Fig. 24, is generated for both bi-lobed and tri-lobed configurations across various shape profiles to assess their aerodynamic performance. This analysis is essential for identifying the shape profile that maximises the lift-to-drag ratio within these configurations. Among the evaluated shape profiles, the tri-lobed model featuring the Garg profile consistently demonstrate superior lift-to-drag ratios over the tested range of angles of attack.

https://doi.org/10.1017/aer.2025.39 Published online by Cambridge University Press

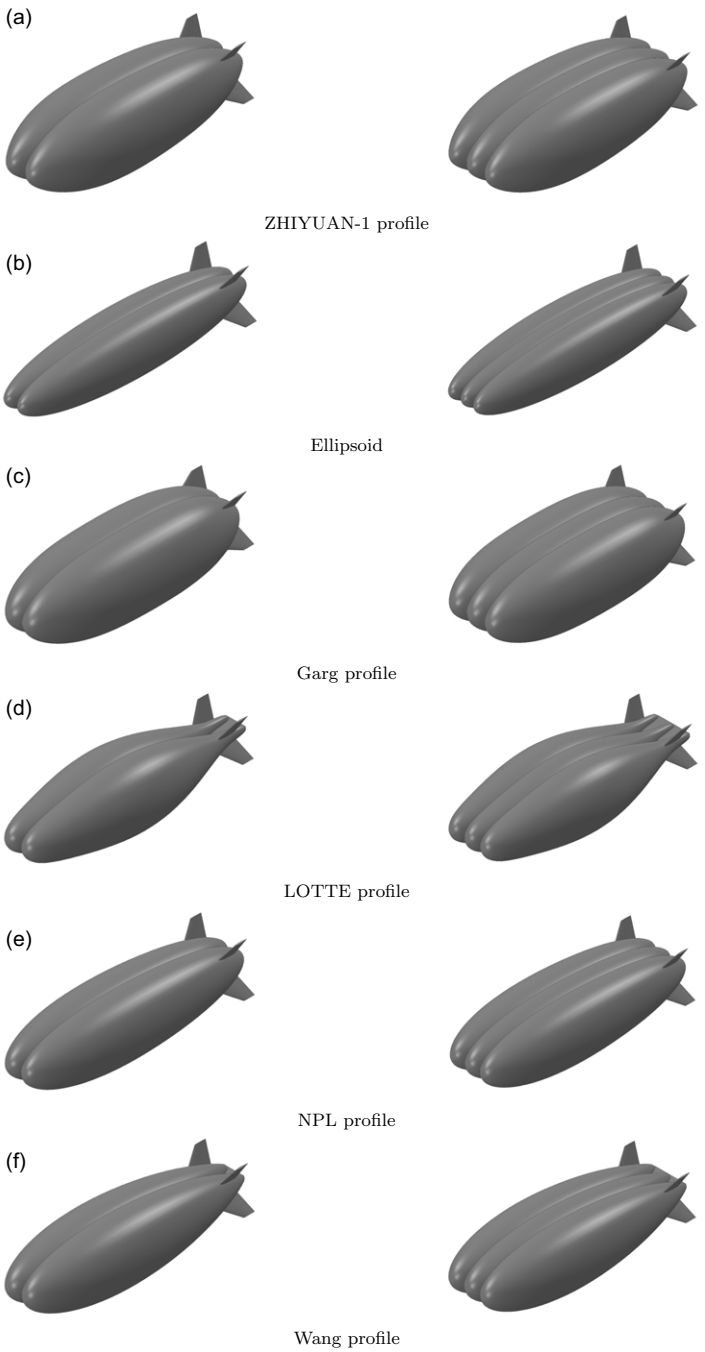

Figure 20. *Multi-lobed configurations.*

Figure 25 compares the aerodynamic characteristics of single-lobed airships (conventional) with multi-lobed airships. An increase of $47-69\%$ in drag coefficient is observed for a bi-lobed configuration compared to a conventional configuration. An even higher increase of $5-6\%$ in drag coefficient is observed for a tri-lobed configuration compared to a bi-lobed one.

https://doi.org/10.1017/aer.2025.39 Published online by Cambridge University Press

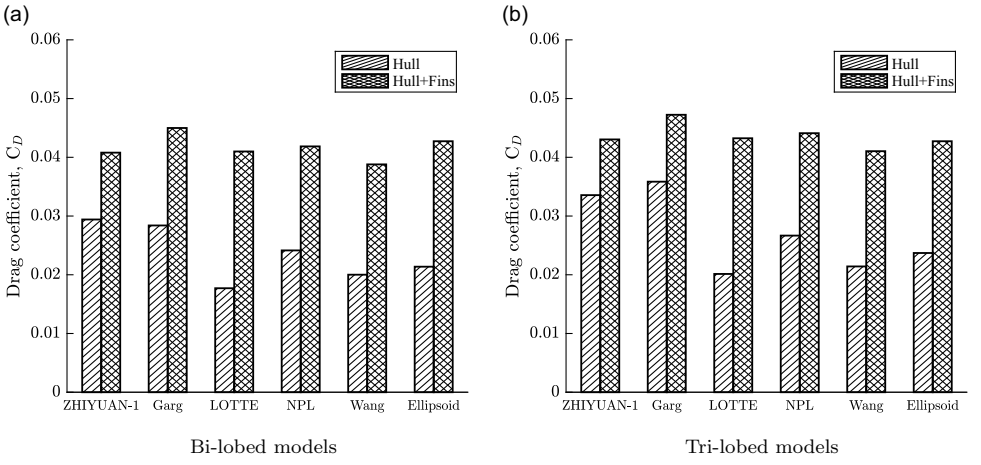

Figure 21. *Comparison of aerodynamic characteristics for multi-lobed airship configurations.*

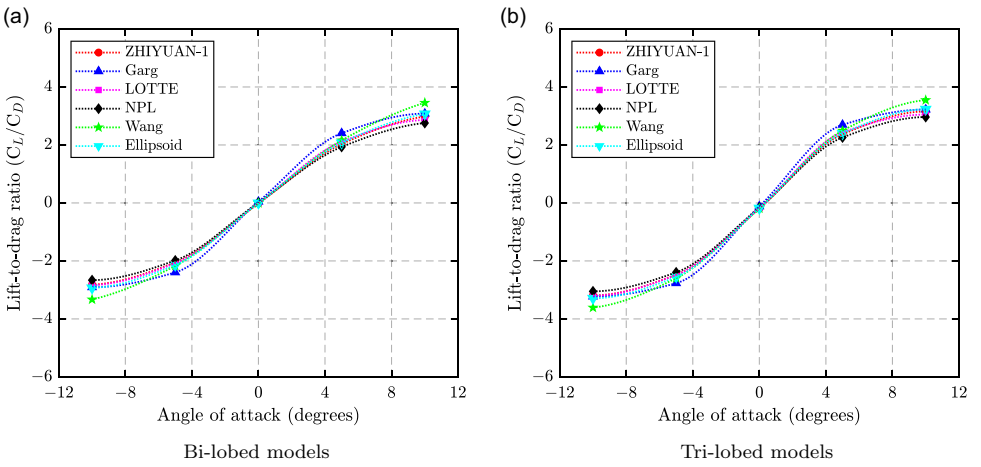

Figure 22. *Aerodynamic efficiency of multi-lobed airship configurations.*

6.0 Conclusions

This study set out to investigate and compare the aerodynamic characteristics of conventional and multi-lobed airship configurations using computational fluid dynamics techniques. The key findings from this research are as follows:

1. The primary aim of this study was to evaluate the aerodynamic performance differences between conventional single-lobed airships and multi-lobed (bi-lobed and tri-lobed) airships.
2. Among the traditional airship designs featuring fins and a gondola, the model incorporating the Wang profile demonstrates a lower drag coefficient than all other models.
3. Multi-lobed airships demonstrated improved aerodynamic efficiency and payload capacity compared to conventional designs. Specifically, they generated significantly more lift for the same hull volume.
4. While multi-lobed airships exhibited higher lift-to-drag ratios, they also experienced increased drag. For instance, bi-lobed configurations showed a $48-118\%$ increase in drag coefficient over conventional designs, and tri-lobed configurations had a further $7-26\%$ increase in drag coefficient compared to bi-lobed designs.

https://doi.org/10.1017/aer.2025.39 Published online by Cambridge University Press

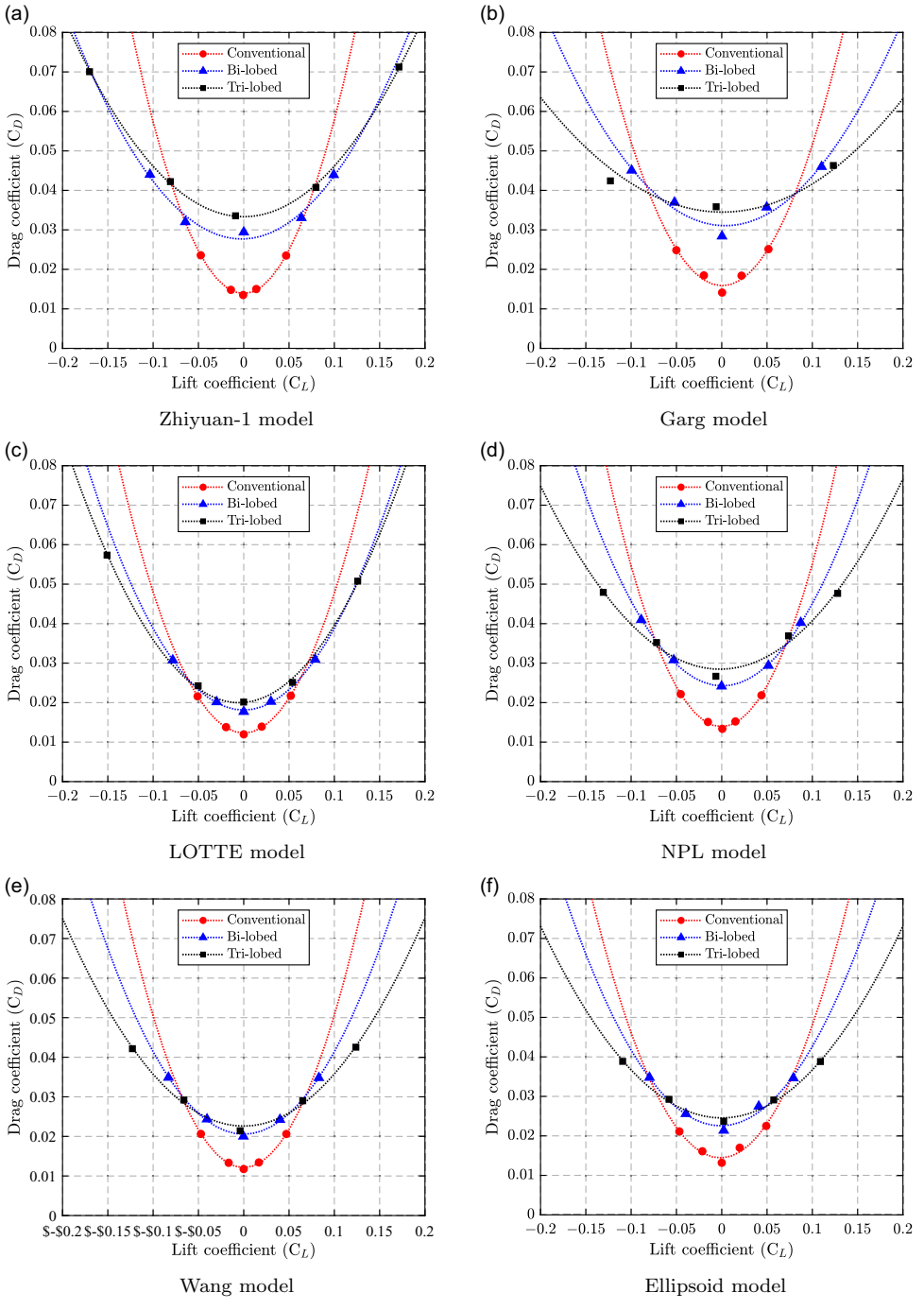

Figure 23. *Drag polar plot.*

5. The addition of fins had a notable effect on aerodynamic performance, improving both lift and drag. The fins were the primary contributors to the increase in drag coefficient, which rose by $28-57\%$ for bi-lobed models and $22-54\%$ for tri-lobed models, significantly impacting the overall lift and drag across all configurations.

https://doi.org/10.1017/aer.2025.39 Published online by Cambridge University Press

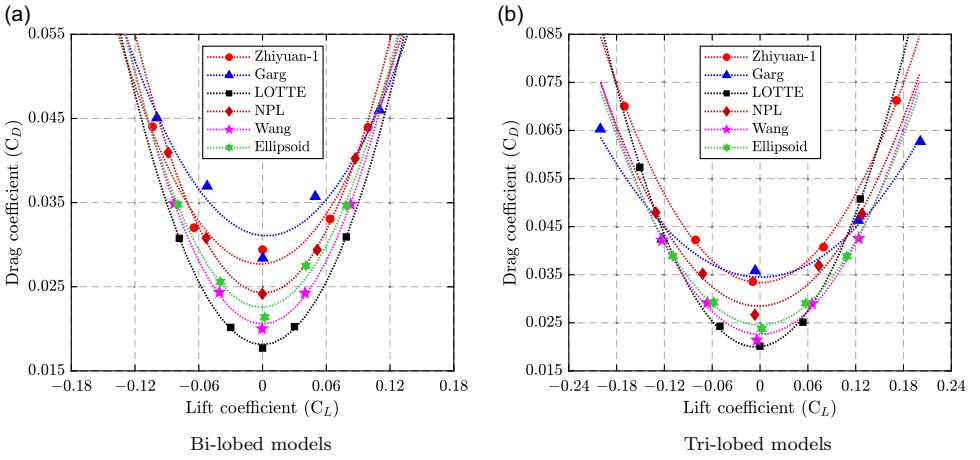

Figure 24. *Drag polar plot for bare hulls.*

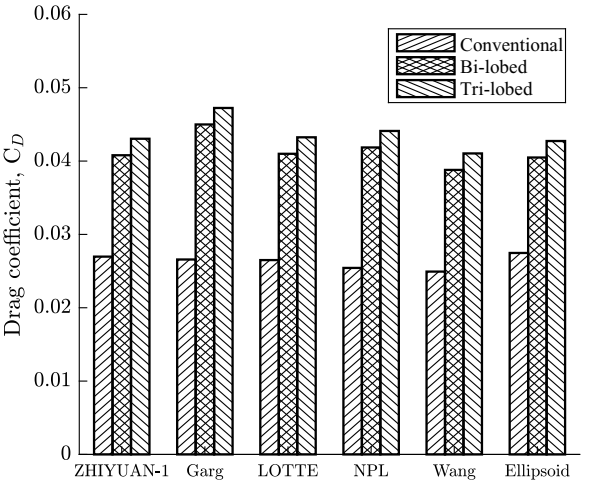

Figure 25. *Comparison between conventional and multi-lobed airships.*

The findings underscore the importance of multi-lobed designs to balance the trade-off between enhanced lift and increased drag. Multi-lobed airships, despite their higher drag, offer better overall aerodynamic efficiency, making them viable for applications requiring higher payload capacity. The improved aerodynamic performance of multi-lobed airships supports their use in diverse applications such as surveillance, cargo transport, and scientific research. The research faced challenges due to the limited availability of experimental data for multi-lobed airship configurations. This constraint necessitates further experimental validation to confirm the CFD results under varied real-world conditions. The simulations were performed under specific conditions and assumptions that might not cover all practical scenarios. Further studies should explore a broader range of operational conditions and configurations. Future research should include extensive experimental testing to validate and refine the CFD models, ensuring their applicability across different operational environments. Exploration of other innovative airship designs and configurations could provide additional insights into optimising aerodynamic performance. Incorporating advancements in materials science, propulsion technologies and control systems could further enhance the performance and efficiency of multi-lobed airships.

This study has demonstrated that multi-lobed airships present a promising alternative to conventional designs, offering substantial improvements in aerodynamic performance. The insights gained from this

https://doi.org/10.1017/aer.2025.39 Published online by Cambridge University Press

research provide a foundation for developing optimised airship designs, contributing to the advancement of green aviation and expanding the potential applications of LTA systems.

7.0 Future scope

1. A more detailed investigation using advanced computational tools should be conducted to supplement the fluid mechanism analysis of the difference in aerodynamic performance between conventional and multi-lobed airships.
2. Since the additional weight of the envelope due to the multi-lobed shape may partially offset the lift gain, this trade-off should be considered.
3. This study focused on C_L and C_D as aerodynamic coefficients, but the impact of multi-lobed tail configurations on aerodynamic stability should be investigated.

Data availability. Some or all data, models or codes that support the findings of this study are available from the corresponding author (Manikandan M.) upon reasonable request.

Acknowledgements. We extend our gratitude to the Manipal Institute of Technology, a part of the Manipal Academy of Higher Education, an Institution of Eminence, for their support and facilitation in the authors' pursuit of knowledge and dissemination of scientific insights. We authors also would like to thank Tamiri Adarsh, and Kanak Agarwal, under-graduate students, Department of Aeronautical and Automobile Engineering, Manipal Institute of Technology, for extending their support in performing the CFD analysis using OpenFOAM software. We would like to acknowledge the National Supercomputing Mission (NSM) for providing us with the computing resources of 'PARAM UTKARSH' at CDAC Knowledge Park, Bengaluru, Karnataka, India which is implemented by C-DAC (Centre for Development of Advanced Computing) and supported by the Ministry of Electronics and Information Technology (MeitY) and the Department of Science and Technology (DST), Government of India.

Author contributions. Conceptualisation – Abhishek Pai and Manikandan M.; Methodology – Abhishek Pai; Software – Abhishek Pai and Manikandan M.; Validation – Abhishek Pai; Writing—original draft preparation – Abhishek Pai; Writing—review and editing – Manikandan M.; Supervision – Manikandan M. All authors have read and agreed to the published version of the manuscript.

Funding statement. This research received no external funding.

Competing interests. The authors declare no conflict of interest.

Institutional review. Not applicable.

Informed consent. Not applicable.

References

[1] Ceruti, A. and Marzocca, P. Conceptual approach to unconventional airship design and synthesis, *J. Aerosp. Eng.*, 2014, **27**, (6), p 04014035.
[2] Agte, J., Gan, T., Kunzi, F., March, A., Sato, S., Suarez, B. and Yutko, B. Conceptual design of a hybrid lift airship for intra-regional flexible access transport, *48th AIAA Aerospace Sciences Meeting Including the New Horizons Forum and Aerospace Exposition*, American Institute of Aeronautics and Astronautics, Inc., 2010, p 1391.
[3] Donaldson, A., Simaiakis, I., Lovegren, J., Pyrgiotis, N., Li, L., Dorbian, C. and He, C. Parametric design of low emission hybrid-lift cargo aircraft, *48th AIAA Aerospace Sciences Meeting Including the New Horizons Forum and Aerospace Exposition*, American Institute of Aeronautics and Astronautics, Inc., 2010, p 1395.
[4] Verma, A.R., Sagar, K.K. and Priyadarshi, P. Optimum buoyant and aerodynamic lift for a lifting-body hybrid airship, *J. Aircraft*, 2014, **51**, (5), pp 1345–1350.
[5] Hartmann, J. Conceptual design of air vehicles with hybrid lift concepts-a design space exploration, *55th AIAA Aerospace Sciences Meeting*, American Institute of Aeronautics and Astronautics, Inc., 2017, p 1625.
[6] Buerge, B. The suitability of hybrid vs. conventional airships for persistent surveillance missions, *48th AIAA Aerospace Sciences Meeting Including the New Horizons Forum and Aerospace Exposition*, American Institute of Aeronautics and Astronautics, Inc., 2010, p 1014.
[7] Zhang, L., Lv, M., Meng, J. and Du, H. Optimization of solar-powered hybrid airship conceptual design, *Aerosp. Sci. Technol.*, 2017, **65**, pp 54–61.

https://doi.org/10.1017/aer.2025.39 Published online by Cambridge University Press

[8] Ceruti, A., Gambacorta, D. and Marzocca, P. Unconventional hybrid airships design optimization accounting for added masses, *Aerosp. Sci. Technol.*, 2018, **72**, pp 164–173.
[9] Manikandan, M. and Pant, R.S. A comparative study of conventional and tri-lobed stratospheric airships, *Aeronaut. J.*, **125**, 2021, (1290), pp 1434–1466.
[10] Sashi Kumar, N., Mahendra, G.A.K. and Raghurama Rao, S.V. Shape optimization using hybrid GA-ACO method and grid-free CFD solver, *18th AIAA Computational Fluid Dynamics Conference*, American Institute of Aeronautics and Astronautics, Inc., 2007, p 3830.
[11] Liu, J.-M., Lu, C.-J. and Xue, L.-P. Numerical investigation on the aeroelastic behavior of an airship with hull-fin configuration, *J. Hydrodyn. Ser. B*, 2010, **22**, (2), pp 207–213.
[12] Suman, S., Lakshmipathy, S. and Pant, R.S. Evaluation of assumed-transition-point criterion in context of reynolds-averaged simulations around lighter-than-air vehicles, *J. Aircr.*, 2013, **50**, (2), pp 450–456.
[13] Mahzan, M.I. and Muhamad, S. An evolution of hybrid airship vehicle (HAV) envelope: aerodynamics analysis, *Appl. Mech. Mater.*, 2014, **660**, pp 498–502.
[14] Andan, A.D, Asrar, W. and Omar, A.A. Investigation of aerodynamic parameters of a hybrid airship, *J. Aircr.*, 2012, **49**, (2), pp 658–662.
[15] Andan, A.D., Asrar, W. and Omar, A.A. Aerodynamics of a hybrid airship, *The 4th International Meeting of Advances in Thermofluids (IMAT 2011), Melaka, Malaysia*, American Institute of Physics, Melville, USA, 2012, 1440, pp 154–161.
[16] Haque, A.U., Asrar, W., Omar, A.A., Sulaeman, E. and Ali, J.M. Conceptual design of a winged hybrid airship, *21st AIAA Lighter-Than-Air Systems Technology Conference*, American Institute of Aeronautics and Astronautics, Inc., 2014, p 2710.
[17] Haque, A.U., Asrar, W., Omar, A.A., Sulaeman, E. and Ali, M.J.S. Effect of side wind on the directional stability and aerodynamics of a hybrid buoyant aircraft, *MATEC Web of Conferences*, EDP Sciences, 2016, 40, p 02006.
[18] Carrión, M., Steijl, R., Barakos, G.N. and Stewart, D. Analysis of hybrid air vehicles using computational fluid dynamics, *J. Aircr.*, 2016, **53**, (4), pp 1001–1012.
[19] Carrion, M., Biava, M., Steijl, R., Barakos, G.N. and Stewart, D. CFD studies of hybrid air vehicles, *54th AIAA Aerospace Sciences Meeting*, American Institute of Aeronautics and Astronautics, Inc., 2016, p 0059.
[20] Carri, M., Biava, M., Steijl, R., et al. Computational fluid dynamics challenges for hybrid air vehicle applications, *Prog. Flight Phys.–Vol. 9*, 2017, **9**, pp 43–80.
[21] Zhang, L., Lv, M., Meng, J. and Du, H. Conceptual design and analysis of hybrid airships with renewable energy, *Proc. Inst. Mech. Eng., Part G: J. Aerosp. Eng.*, 2018, **232**, (11), pp 2144–2159.
[22] Reddy, M.D. and Pant, R.S. CFD analysis of axisymmetric bodies of revolution using openfoam, *2018 Applied Aerodynamics Conference*, American Institute of Aeronautics and Astronautics, Inc., 2018, p 3334.
[23] Meng, J., Li, M., Zhang, L., Lv, M. and Liu, L. Aerodynamic performance analysis of hybrid air vehicles with large reynolds number, *2019 IEEE International Conference on Unmanned Systems (ICUS)*, IEEE, New York, USA, 2019, pp 403–409.
[24] Yang, Y., Xu, X., Zhang, B., Zheng, W. and Wang, Y. Bionic design for the aerodynamic shape of a stratospheric airship, *Aerosp. Sci. Technol.*, 2020, **98**, p 105664.
[25] Gupta, P., Tripathi, M. and Pant, R.S. Aerodynamic analysis of axi-symmetric lighter-than-air vehicles, *AIAA Aviation 2021 Forum*, American Institute of Aeronautics and Astronautics, Inc., 2021, p 2987.
[26] Anoop, S., Velamati, R.K. and Oruganti, V.R.M. Aerodynamic characteristics of an aerostat under unsteady wind gust conditions, *Aerosp. Sci. Technol.*, 2021, **113**, p 106684.
[27] Sasidharan, A., Velamati, R.K., Janardhanan, S., Oruganti, V.R.M. and Mohammad, A. Stability derivatives of various lighter-than-air vehicles: a CFD-based comparative study, *Drones*, 2022, **6**, (7), p 168.
[28] Magar, A., Gulawani, S.S., Kiran Babu, K.M. and Pant, R.S. Numerical investigation of laminar to turbulent boundary layer transition over airship envelopes, *Lighter Than Air Systems: Proceedings of the International Conference on Design and Engineering of Lighter-Than-Air Systems 2022 (DELTAs-2022)*, Springer, India, 2022, pp 167–181.
[29] Zhang, L., Li, J., Meng, J., Du, H., Lv, M. and Zhu, W. Thermal performance analysis of a high-altitude solar-powered hybrid airship, *Renew. Energy*, 2018, **125**, pp 890–906.
[30] Zhang, L., Lv, M., Zhu, W., Du, H., Meng, J. and Li, J. Mission-based multidisciplinary optimization of solar-powered hybrid airship, *Energy Convers. Manag.*, 2019, **185**, pp 44–54.
[31] Funk, P., Lutz, T. and Wagner, S. Experimental investigations on hull-fin interferences of the Lotte airship, *Aerosp. Sci. Technol.*, 2003, **7**, (8), pp 603–610.
[32] Liu, P., Fu, G.-Y., Zhu, L.-J. and Wang, X.-L. Aerodynamic characteristics of airship zhiyuan-1, *J. Shanghai Jiaotong Univ. (Sci.)*, 2013, **18**, pp 679–687.
[33] Lindow, S.S., Kulhanek, N.E., Richardson, N.M., Schroeder, B.E. and Buerge, B. An experimental investigation of hybrid airships, *2023 Regional Student Conferences*, American Institute of Aeronautics and Astronautics, Inc., 2023, p 72073.
[34] Yanxiang, C., Yanchu, Y., Jianghua, Z., et al. Numerical aerodynamic investigations on stratospheric airships of different tail configurations, *2015 IEEE Aerospace Conference*, IEEE, New York City, U.S., 2015, pp 1–9.
[35] Mendonça, Jr., J.L., Santos, J.S., Morales, M.A., Goes, L.C., Stevanovic, S. and Santana, R.A. Airship aerodynamic coefficients estimation based on computational method for preliminary design, *AIAA Aviation 2019 Forum*, American Institute of Aeronautics and Astronautics, Inc., 2019, p 2982.
[36] Akbari, A., Noori, S. and Spahvand, P. A numerical investigation on the roll damping coefficient of a typical airship based on the computational fluid dynamics, *J. Aerosp. Sci. Technol.*, 2021, **14**, (2), pp 10–18.
[37] Suvarna, S., Chung, H., Sinha, A. and Pant, R.S. Revised semi-empirical aerodynamic estimation for modelling flight dynamics of an airship, *Aerosp. Sci. Technol.*, 2022, **126**, p 107642.

https://doi.org/10.1017/aer.2025.39 Published online by Cambridge University Press

[38] Suvarna, S., Chung, H. and Pant, R.S. Optimization of fins to minimize directional instability in airships, *J. Aircr.*, 2022, **59**, (2), pp 317–328.
[39] Voloshin, V., Chen, Y.K. and Calay, R.K. A comparison of turbulence models in airship steady-state CFD simulations, *arXiv preprint arXiv:1210.2970*, 2012.
[40] El Omari, K., Schall, E., Koobus, B. and Dervieux, A. Turbulence modeling challenges in airship CFD studies, *Monografas del SeminarioMatemáticoGarca de Galdeano*, 2004, **31**, pp 545–554.
[41] El Omari, K., Schall, E., Le Guer, Y. and Amara, M. Numerical study of turbulent flow around a generic airship at high angle of attack, *4th International Conference on Computational Heat and Mass Transfer*, Paris-Cachan, France, May 17–20, 2005.
[42] Wu, X.-C., Wang, Y.-W., Huang, C.-G., Du, T.-Z., Yu, X.-X. and Liao, L.-J. Aerodynamic simulation of airship ambient flows with high attack angles and analysis on turbulence models and parameters, *Eng. Mech.*, 2014, **31**, (8), pp 24–31.
[43] Kanoria, A.A., Panchal, K., Dongre, R. and Damodaran, M. Computational modelling of aerodynamic characteristics of airships in arbitrary motion, *22nd AIAA Lighter-Than-Air Systems Technology Conference*, American Institute of Aeronautics and Astronautics, Inc., 2015, p 3230.
[44] Tripathi, M., Murugaiah, M., Pandey, P. and Pant, R.S. Drag mitigation of trilobed airship hull through aerodynamic comparison with conventional single-lobed hull, *J. Aerosp. Eng.*, 2023, **36**, (6), p 04023073.
[45] Gertler, M. *Resistance Experiments on a Systematic Series of Streamlined Bodies of Revolution: For Application to the Design of High-Speed Submarines*. Navy Department, David W. Taylor Model Basin, Washington, DC, 1950.
[46] Landweber, L. and Gertler, M. *Mathematical Formulation of Bodies of Revolution*. Navy Department, David W. Taylor Model Basin, Washington, DC, 1950.
[47] Alam, M.I. and Pant, R.S. Surrogate based shape optimization of airship envelopes, *24th AIAA Aerodynamic Decelerator Systems Technology Conference*, American Institute of Aeronautics and Astronautics, Inc., 2017, p 3393.
[48] Manikandan, M., Shah, R.R., Priyan, P., Singh, B. and Pant, R.S. A parametric design approach for multi-lobed hybrid airships, *Aeronaut. J.*, 2024, **128**, (1319), pp 1–36.
[49] Wang, X.-L., Fu, G.-Y., Duan, D.-P. and Shan, X.-X. Experimental investigations on aerodynamic characteristics of the zhiyuan-1 airship, *J. Aircr.*, 2010, **47**, (4), pp 1463–1468.
[50] Agarwal, K., Vijaykrishnan, V., Mohanty, D. and Murugaiah, M. A comprehensive dataset of the aerodynamic and geometric coefficients of airfoils in the public domain, *Data*, 2024, **9**, (5), p 64.
[51] Carichner, G.E. and Nicolai, L.M. Fundamentals of aircraft and airship design, *Volume 2–Airship Design and Case Studies*, American Institute of Aeronautics and Astronautics, Inc., Reston, VA, USA, 2013.
[52] Tripathi, M., Misra, A. and Sucheendran, M.M. Effect of planar member cross-section on cascade fin aerodynamics, *J. Spacecr. Rockets*, 2019, **56**, (3), pp 744–760.
[53] Spalart, P. and Allmaras, S. A one-equation turbulence model for aerodynamic flows, *30th Aerospace Sciences Meeting and Exhibit*, American Institute of Aeronautics and Astronautics, Inc., 1992, p 439.
[54] Dacles-Mariani, J., Zilliac, G.G., Chow, J.S. and Bradshaw, P. Numerical/experimental study of a wingtip vortex in the near field, *AIAA J.*, 1995, **33**, (9), pp 1561–1568.
[55] Menter, F. Zonal two equation k-w turbulence models for aerodynamic flows, *23rd Fluid Dynamics, Plasmadynamics, and Lasers Conference*, American Institute of Aeronautics and Astronautics, Inc., 1993, p 2906.
[56] Menter, F.R. Two-equation eddy-viscosity turbulence models for engineering applications, *AIAA J.*, 1994, **32**, (8), pp 1598–1605.
[57] Jones, W.P. and Launder, B.E. The prediction of laminarization with a two-equation model of turbulence, *Int. J. Heat Mass Transf.*, 1972, **15**, (2), pp 301–314.
[58] Launder, B.E. and Sharma, B.I. Application of the energy-dissipation model of turbulence to the calculation of flow near a spinning disc, *Lett. Heat Mass Transf.*, 1974, **1**, (2), pp 131–137.

Cite this article: Pai A. and Manikandan M. (2025). A comparative study of aerodynamic characteristics of conventional and multi-lobed airships. *The Aeronautical Journal*, **129**, 2435–2459. https://doi.org/10.1017/aer.2025.39